STEM CELLS

Copy of e-mail Notification

STEM CELLS Co-Published by AlphaMed Press and Wiley-Blackwell

Dear Author,

YOUR PAGE PROOFS ARE AVAILABLE IN PDF FORMAT; please refer to this URL address
http://115.111.50.156/jw/retrieval.aspx?pwd=256b663e6525

You will be prompted to log in, and asked for a password. Your login name will be your email address password will be
Password: 256b663e6525

You will need to have Adobe Acrobat Reader software to read these files. This is free software and is available for user downloading at http://www.adobe.com/products/acrobat/readstep.html.

The site contains one PDF file, that contains the following:

- Annotated PDF Instructions
- Reprint Order Information
- Publication Fee Form
- A copy of your page proofs for your article

Please read the page proofs carefully and:

1) indicate changes or corrections using the Annotated editing instructions at the front of the page proof packet;
2) answer all queries
3) proofread any tables and equations carefully;
4) check that any special characters have translated correctly.
5) check your figure(s) and legends for accuracy
6) complete Publication Fee Form and return with page proof corrections, if not previously returned.

Special Notes:

We strongly encourage authors to correct proofs by annotating PDF files. Any corrections should be returned to jrnlprod.STEM@cenveo.com within 2 business days after receipt of this email. Thank you for your cooperation.

Stem Cells is covered by Wiley’s Early View service, which means that once we have received your corrections, your article will be published online without having to wait for inclusion in a paginated issue. Please note that the version of your paper that appears online is complete and final, except for volume, issue and page numbers, which are added upon issue publication. Therefore, there will be no further opportunity to make changes to your article after online publication.

STEM CELLS

Copy of e-mail Notification

Production Editor, STEM
E-mail: jrnlprod.STEM@cenveo.com

Technical problems? If you experience technical problems downloading your file or any other problem with the website listed above, please contact cs.wiley@cenveo.com, phone:+91 (44) 4205 8810.

Questions regarding your article? Trouble interpreting any of the questions listed at the end of your file?

REMEMBER TO INCLUDE YOUR ARTICLE NO. (2210) WITH ALL CORRESPONDENCE. This will enable us to address your query more efficiently.

As this e-proofing system was designed to make the publishing process easier for everyone, we welcome any and all feedback. Thanks for participating in our e-proofing system!

This e-proof is to be used only for the purpose of returning corrections to the publisher.

Sincerely,
Production Editor, STEM
E-mail: jrnlprod.STEM@cenveo.com

WILEY-BLACKWELL

USING e-ANNOTATION TOOLS FOR ELECTRONIC PROOF CORRECTION

Required software to e-Annotate PDFs: Adobe Acrobat Professional or Adobe Reader (version 8.0 or above). (Note that this document uses screenshots from Adobe Reader X)
The latest version of Acrobat Reader can be downloaded for free at: http://get.adobe.com/reader/

Once you have Acrobat Reader open on your computer, click on the Comment tab at the right of the toolbar:

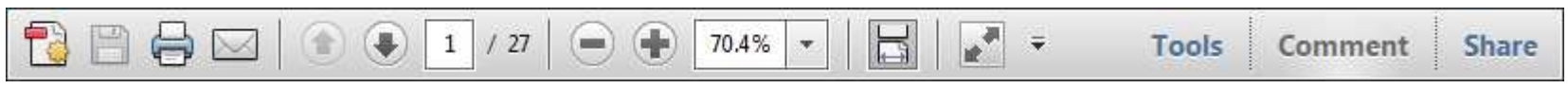

This will open up a panel down the right side of the document. The majority of tools you will use for annotating your proof will be in the Annotations section, pictured opposite. We've picked out some of these tools below:

1. Replace (Ins) Tool – for replacing text.

Strikes a line through text and opens up a text box where replacement text can be entered.

How to use it

- Highlight a word or sentence.
- Click on the Replace (Ins) icon in the Annotations section.
- Type the replacement text into the blue box that appears.

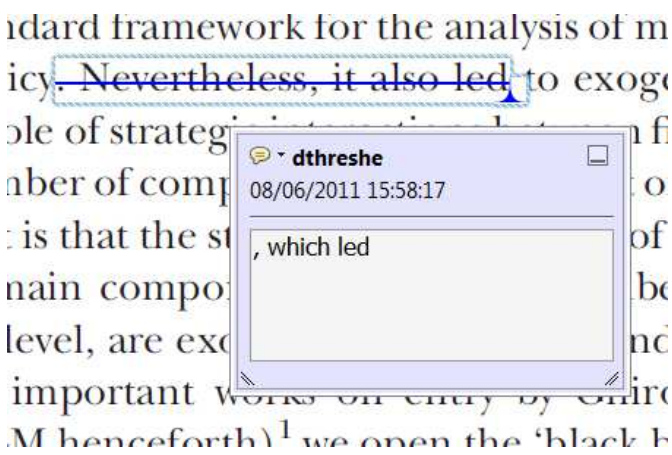

2. Strikethrough (Del) Tool – for deleting text.

Strikes a red line through text that is to be deleted.

How to use it

- Highlight a word or sentence.
- Click on the Strikethrough (Del) icon in the Annotations section.

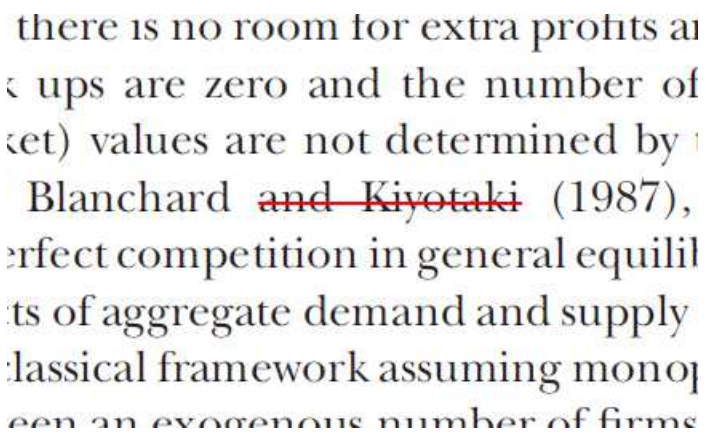

3. Add note to text Tool – for highlighting a section to be changed to bold or italic.

Highlights text in yellow and opens up a text box where comments can be entered.

How to use it

- Highlight the relevant section of text.
- Click on the Add note to text icon in the Annotations section.
- Type instruction on what should be changed regarding the text into the yellow box that appears.

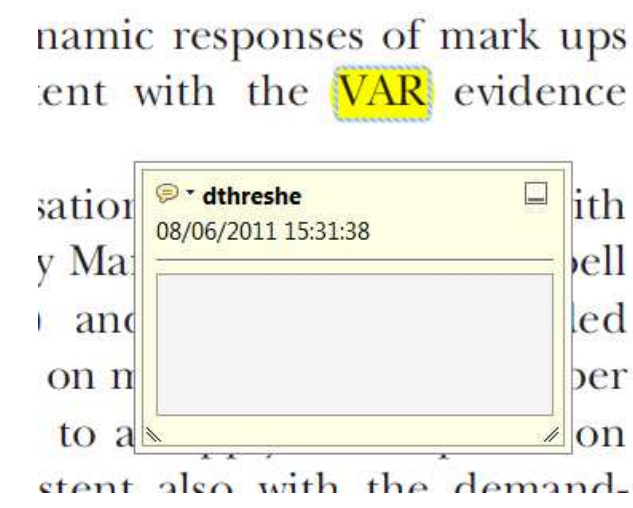

4. Add sticky note Tool – for making notes at specific points in the text.

Marks a point in the proof where a comment needs to be highlighted.

How to use it

- Click on the Add sticky note icon in the Annotations section.
- Click at the point in the proof where the comment should be inserted.
- Type the comment into the yellow box that appears.

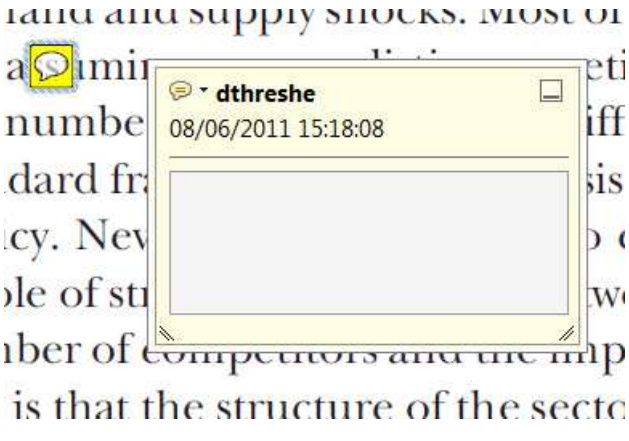

WILEY-BLACKWELL

USING e-ANNOTATION TOOLS FOR ELECTRONIC PROOF CORRECTION

5. Attach File Tool – for inserting large amounts of text or replacement figures.

Inserts an icon linking to the attached file in the appropriate pace in the text.

How to use it

- Click on the Attach File icon in the Annotations section.
- Click on the proof to where you'd like the attached file to be linked.
- Select the file to be attached from your computer or network.
- Select the colour and type of icon that will appear in the proof. Click OK.

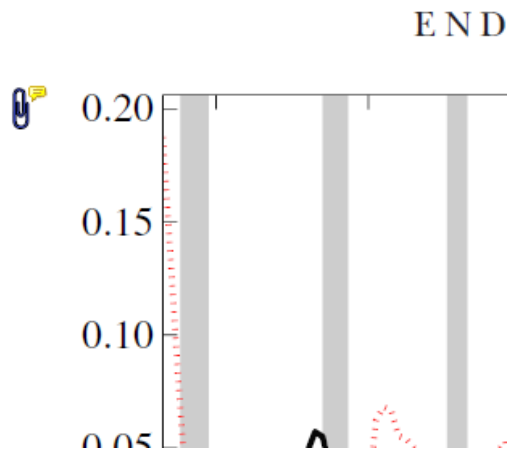

6. Add stamp Tool – for approving a proof if no corrections are required.

Inserts a selected stamp onto an appropriate place in the proof.

How to use it

- Click on the Add stamp icon in the Annotations section.
- Select the stamp you want to use. (The Approved stamp is usually available directly in the menu that appears).
- Click on the proof where you'd like the stamp to appear. (Where a proof is to be approved as it is, this would normally be on the first page).

7. Drawing Markups Tools – for drawing shapes, lines and freeform annotations on proofs and commenting on these marks.

Allows shapes, lines and freeform annotations to be drawn on proofs and for comment to be made on these marks..

How to use it

- Click on one of the shapes in the Drawing Markups section.
- Click on the proof at the relevant point and draw the selected shape with the cursor.
- To add a comment to the drawn shape, move the cursor over the shape until an arrowhead appears.
- Double click on the shape and type any text in the red box that appears.

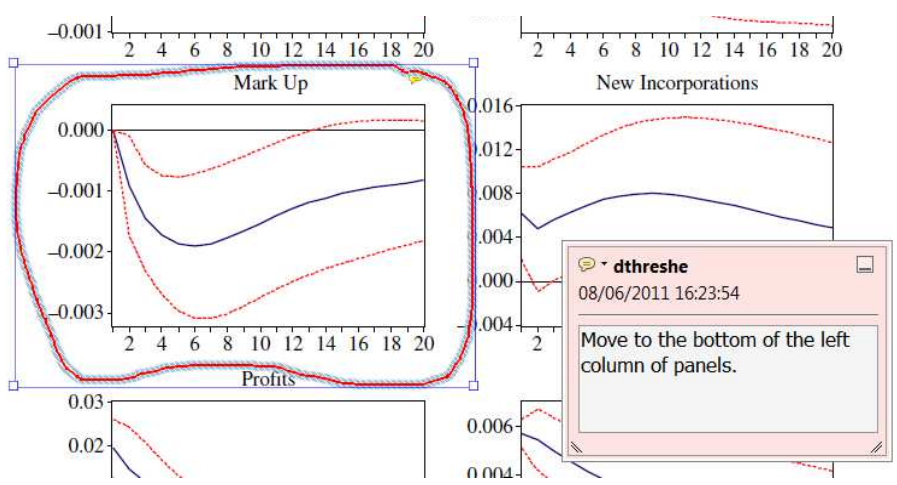

For further information on how to annotate proofs, click on the Help menu to reveal a list of further options:

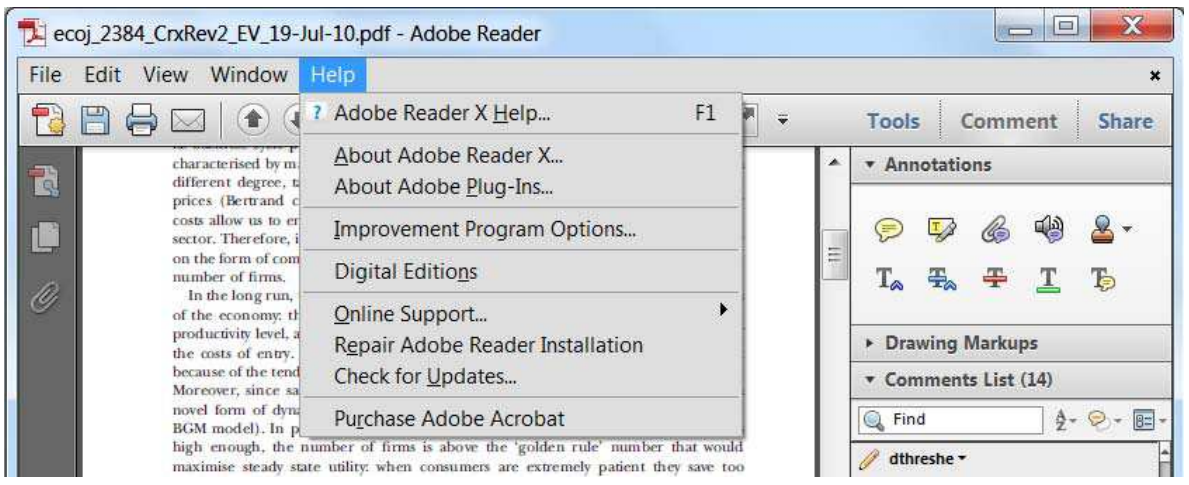

STEM CELLS®

WILEY-BLACKWELL
AlphaMed Press

PUBLICATION FEE FORM

Proffered manuscripts that are accepted for publication will be assessed a publication fee of $2,000, which includes all page charges and any applicable color charges. The author agrees to pay this fee to the Publisher within 30 days of receiving the Publisher's invoice. If an author is unable to support this publication fee, it is his or her responsibility to inform the Publisher at the time of manuscript submission. (Letters to the Editor and invited manuscripts are exempt from the publication fee.)

Please return this form with your corrected proofs to: Production Editor, e-mail: jrnlprod.STEM@cenveo.com

JOURNAL **Stem Cells** VOLUME _____ ISSUE _____

TITLE OF MANUSCRIPT _____

MS. NO. _____ NO. OF PAGES_____ AUTHOR(S) _____

***Invited material is not subject to publication charges**.*

Flat Publication Fee $ 2000.00 US

International orders must be paid in currency and drawn on a U.S. bank

Please check one: ☐ Check enclosed ☐ Bill me

BILL TO:

Name _____

Institution _____

Address _____

_____

_____

Phone: _____ Fax: _____

E-mail: _____

STEM CELLS®

REGENERATIVE MEDICINE

Molecular and Cellular Functions Distinguish Superior Therapeutic Efficiency of Bone Marrow CD45 Cells Over Mesenchymal Stem Cells in Liver Cirrhosis

AQ8

PRAKASH BALIGAR,[a] SNEHASISH MUKHERJEE,[a] VEENA KOCHAT,[a] ARCHANA RASTOGI,[b] ASOK MUKHOPADHYAY[a]

Key Words. Hematopoietic cells • Hepatic stellate cells • Liver fibrosis • Liver regeneration • Macrophages

[a]Stem Cell Biology Laboratory, National Institute of Immunology, New Delhi, India; [b]Department of Pathology, Institute of Liver & Biliary Sciences, Vasant Kunj, New Delhi, India

AQ1

Correspondence: Asok Mukhopadhyay, Ph.D., National Institute of Immunology, Aruna Asaf Ali Marg, New Delhi 110067, India. Telephone: 91-11-26715004; Fax: 91-11-26742125; e-mail: ashok@nii.ac.in

Received June 18, 2015; accepted for publication August 24, 2015; first published online in STEM CELLS *EXPRESS* Month 00, 2015.

1066-5099/2014/$30.00/0

http://dx.doi.org/10.1002/stem.2210

ABSTRACT

Liver fibrosis is strongly associated with chronic inflammation. As an alternative to conventional treatments for fibrosis, mesenchymal stem cells (MSCs) therapy is found to be attractive due to its immunomodulatory functions. However, low survival rate and profibrogenic properties of MSCs remain the major concerns, leading to skepticism in many investigators. Here, we have asked the question whether bone marrow (BM)-derived CD45 cells are the better candidate than MSCs to treat fibrosis, if so, what are the molecular mechanisms that make such distinction. Using CCl_4-induced liver fibrosis mouse model of a Metavir fibrosis score 3, we showed that BM-CD45 cells have better antifibrotic effect ~~that~~ adipose-derived (AD)-MSCs. In fact, our study revealed that antifibrotic potential of CD45 cells are compromised by the presence of MSCs. This difference was apparently due to significantly high level expressions of matrix metalloproteinases-9 and 13, and the suppression of hepatic stellate cells' (HpSCs) activation in the CD45 cells transplantation group. Mechanism dissection studied in vitro supported the above opposing results and revealed that CD45 cell-secreted FasL induced apoptotic d[illegible]of activated HpSCs. Further [illegible]ses suggest that MSC-secreted transforming growth factor β and insulin-like growth factor-1 promoted myofibroblastic differentiation of HpSCs and their proliferation. Additionally, the transplantation of CD45 cells led to functional improvement of the liver through repair and regeneration. Thus, BM-derived CD45 cells appear as a superior candidate for the treatment of liver fibrosis due to structural and functional improvement of CCl_4-induced fibrotic liver, which were much lower in case of AD-MSC therapy. STEM CELLS *2015; 00:000–000*

SIGNIFICANCE STATEMENT

During past 10 years, mesenchymal stem cells (MSCs) has been given highest priority to treat fibrotic liver due to immunosuppressive properties. Despite of that, use of MSCs to treat fibrosis is not beyond any scrutiny, as we have shown that MSCs generate cues for myofibroblastic differentiation and anti-apoptosis of stellate cells, and prevent scar-associated macrophages to degrade ECM. In the present manuscript, we have shown that CD45 cells induce apoptotic death of stellate cells, prevent their myofibroblastic differentiation and facilitate degradation of scar, involve in repair and regeneration of liver in mouse. In clinical translation, CD45 cell therapy is believed to be most appropriate as these cells can be easily harvested and transfused, and no culture manipulation is required for that. Because large number of CD45 cells can be harvested from patientã s cytokine mobilized peripheral blood, less invasive technique than bone marrow harvest can be adopted for this purpose.

INTRODUCTION

Chronic liver injury (CLI) by any toxic insult or viral infections results in scar deposition leading to cirrhosis, which impedes the normal function of the liver and its regeneration. Cirrhotic livers often develop hepatocellular carcinoma [1]. End-stage patients are treated with orthotopic liver transplantation, which may improve the survival rate by 5 years [2]; however, many of them show adverse side effects like infection and multiorgan failure due to prolong usage of immunosuppressive drugs. Furthermore, the treatment of end-stage liver disease is limited due to global shortage of cadaver/donor organ,

J_ID: STEM Customer A_ID: STEM2210 Cadmus Art: STEM2210 Ed. Ref. No.: 15-0505.R1 Date: 24-September-15 Stage: Page: 2

which encourages the development of alternate strategies to treat cirrhotic liver.

CLI is marked by persistence inflammation, in which monocytes/macrophage play a central role. As a consequence to inflammation, transforming growth factor β (TGFβ) pathway activation in hepatic stellate cells (HpSCs) results in myofibroblastic differentiation, leading to the formation of scar. Therefore, mainly two alternate strategies are generally followed to improve the prognosis of the disease: targeting TGFβ pathway and suppressing inflammation [3–5].

In recent past, many clinical trials have been conducted for treatment of cirrhotic liver, mostly using mesenchymal stem cells (MSCs) [6–10]. Although these studies have registered some clinical improvement without severe side effects, the long-term benefits remain uncertain. The main purpose of using MSCs was due to their immunosuppressive properties, which can take care of sustained inflammation in case of liver fibrosis [7, 8]. In a mouse model of CLI, treatment with MSCs resulted in suppression of hepatic infiltration of immune cells, reducing liver fi [9, 10]. However, resent studies proposed that in CLI the regression of fibrosis is associated with differentiation of proinflammatory macrophages into resident type that secrete matrix metalloproteinases (MMPs) to degrade scar [11–13]. This was partly supported by earlier studies where resolution of CCl_4-induced liver fibrosis was found to be abrogated leading to scar formation due to the selective depletion of scar-associated macrophages (SAM) or the use of MMP13-deficient mice to create fibrosis [14, 15]. These findings encouraged the use of bone marrow (BM)-derived activated macrophages for the treatment of liver fibrosis in mice [16]. Hence, the most critical question that emerges is whether the suppression of chronic hepatic inflammation is desirable for the treatment of fibrosis in all stages? Furthermore, MSCs were found to be profibrogenic, not only because they secrete fibrogenic molecules [17], but also because they can directly differentiate into myofibroblasts in experimental mouse model of liver fibrosis as well as in patients [18, 19]. Therefore, it is necessary to explore the antifibrotic potential of BM cells, other than MSCs. Additionally, it is obligatory to evaluate the paracrine role of MSCs in terms of the protection or induction of apoptosis in activated HpSCs, to see whether the secreted factors promote or inhibit myofibroblastic differentiation. Unless these questions are addressed, the treatment by BM cells or MSCs may prove detrimental to the patients.

In this study, we have compared the antifibrotic role of BM-derived CD45 cells with adipose-derived (AD)-MSCs in CCl_4-induced liver fibrosis model. Specifically, we investigated whether these two cell types influence the HpSCs differently, and if so, what is the cellular and molecular mechanism of fibrosis resolution. Our results suggest that BM-CD45 cells therapy ameliorated fibrosis and regenerated liver more efficiently than MSCs.

Materials and Methods

Animals

Six- to eight-week-old male C57BL/6J and enhanced green fluorescence protein (eGFP) transgenic mice (C57BL/6-Tg(UBC-GFP)$_{30}$Scha/J) were used in this investigation. Mice were obtained from Jackson Laboratories (Bar Harbor, ME) and maintained in an experimental animal facility in our institute. Mice were kept in an individual ventilated cages and fed with autoclaved acidified water and irradiated food ad libitum. All experiments were conducted as per procedures approved by the Institutional Animal Ethics Committee at the National Institute of Immunology, New Delhi, India.

Experimental Liver Fibrosis Model and Transplantation

A liver fibrosis model was established in C57Bl6/J mice by repeated injection of CCl_4 (0.8 ml/kg b.wt.) in mineral oil, twice a week, for a period of 8 weeks (16 doses) via the intraperitoneal route till a Metavir score 3 was achieved [20]. Sixty such mice were divided equally three groups. Group A (sham control, ShC) mice received PBS. Group B (Tx_{CD45}) and Group C (Tx_{MSC}) mice received 5×10^6 BM-CD45 cells (freshly isolated) and 0.25×10^6 AD-MSCs (passage 3) per mouse, respectively, from eGFP transgenic mice through intrasplenic route. Low transplantation dose of AD-MSCs was due to their large size (35–40 μm) as compared to BM-CD45 cells. We could not perform this comparative study using higher dose of MSCs, as at increasing cell number (0.5×10^6 MSCs/mouse) the mortality of mice was approximately 80%. These three groups of mice were given additional doses of CCl_4 (eight doses) to maintain a profibrotic environment. A separate transplantation experiment was conducted following above protocol in which CD45 cells or MSCs or together were delivered in fibrotic liver. After 4 weeks of transplantation, mice were sacrificed, livers were isolated to examine for fibrosis and gene expression, and sera were stored for liver function tests. The extent of fibrosis was determined by staining with picrosirius red (Polyscience, Inc., PA), followed by determining the collagen proportionate area (CPA) using Image J software (NIH). The activation status of HpSCs was examined by staining with alpha-smooth muscle actin (α-SMA) antibody, followed by determining the α-SMA area as explained above. The presence of SAM in fibrotic zone was identified by costaining sections with matrix metalloproteinase (MMP)−13 antibody and picrosirius red.

Isolation and Characterization of Cells

Mononuclear BM cells of eGFP transgenic female mice were stained with mouse anti-CD45/APC (1:200, cat# 17–0451, BD Bioscience, San Diego, CA) and then sorted for $CD45^+$ cells using FACS AriaIII (BD Bioscience). BM-derived CD45 cells were phenotypically characterized for the presence of monocytes/macrophages (CD11b and F4/80), hematopoietic stem (LSK), uncommitted cells (Lin^-), and NK ($CD56^+CD3^-$) cells by immunostaining (Supporting Information Methods and Supporting Information Fig. SF1). AD-MSCs were isolated from abdominal fat of the same mouse following a published protocol [21]. In brief, fat tissue was digested with collagenase, the cells were cultured in low glucose Dulbecco's modified Eagle's medium supplemented with 10% FBS for 2 days. The trypsinized cells were subcultured (3,000 cells per square centimeter) for consecutive three passages before phenotypically characterized (Supporting Information Methods and Supporting Information Fig. SF2).

Culture of HpSCs with Conditioned Media

HpSCs were isolated from 8 weeks post-treated fibrotic liver (Supporting Information Methods), 5.0×10^4 cells were

ID: parasuramank Time: 12:52 I Path: //chenas03/Cenpro/ApplicationFiles/Journals/Wiley/STEM/Vol00000/150206/Comp/APPFile/JW-STEM150206

J_ID: STEM Customer A_ID: STEM2210 Cadmus Art: STEM2210 Ed. Ref. No.: 15-0505.R1 Date: 24-September-15 Stage: Page: 3

placed on each poly(L-lysine)-coated cover slip, and separately cultured in 5% FBS supplemented Ham F-12 medium or with 1:1 diluted CD45 or MSC-conditioned medium (CM) for 72 and 120 hours. Conditioned media were prepared by growing either 2×10^6 CD45 cells or AD-MSCs for 2 days in 10 ml of serum supplemented medium. In separate experiments, HpSCs were cultured as above, but in the presence or absence of 50 μM SB-431542 (Cayman Chemical, MI) to determine the effect of inhibition of TGFβ pathway on myofibroblastic differentiation. A bioneutralization assay of FasL was conducted in a 48-well plate by incubating 5.0×10^4 cells in 1:1 diluted conditioned media as such (control) or preincubated with an anti-FasL antibody (R&D Systems, Minneapolis, MN). Depending upon the nature of the experiments, the aHpSCs were analyzed for proliferation/inhibition (MTT assay and Ki67 staining), apoptosis (Caspase-3/7 Assay), myofibroblastic differentiation (αSMA and collagen-1α expression), and gene expression (RT-PCR).

Immunohistochemistry and Immunocytochemistry

Four percentage PFA-fixed liver tissues were frozen in tissue freezing medium (Jung, Leica Microsystems, Germany). Five micron sections were cut and treated with 0.15% Triton X-100 for 30 minutes in room temperature. Similarly, 4% PFA-fixed cells were treated with 0.15% Triton X-100 for 30 minutes in room temperature. The sections or cells were stained with different antibodies for 1 hour. After three times washing, tissue sections/cells were reacted with secondary antibodies conjugated with the flurochromes for another 1 hour. The sections were further washed and the nuclei were stained with 4′,6-diamidino-2-phenylindole. The sections were imaged using Olympus fluorescence microscope (Olympus, Tokyo) using LCPlanFl ×20 and ×60 objectives. Images were also captured using Leica SP5 II confocal laser-scanning microscope with Plan-Apochromat ×63/1.4 oil objective and LAS/AF Lite software for analysis. The images were composed and edited in Photoshop 6.0 (Adobe). The antibodies used were anti-mouse CK18 (1:200, cat# sc-32329), anti-mouse CK19 (1:50, cat# sc-25724), and anti-human MMP13 (1:200, cat# sc-30073) from Santa Cruz Biotechnology (Santa Cruz, CA), anti-mouse α-SMA (1:200, cat# IMG-80014, Imgenex, Bhubaneswar, India), rabbit polyclonal anti-α-SMA (1:200, cat# ab 5694, Abcam, Cambridge, U.K.), anti-desmin (1:100, cat# 46–777, Prosci, Inc., Poway, CA), anti-mouse eGFP (1:250, cat# 632381, Clontech-Takara Bio Company, Kyoto, Japan), anti-mouse albumin (1:100, cat# A90–134A, Bethyl, Montgomery, TX), anti-mouse Ki67 (1:50, cat# ab15580, Abcam), and collagen-1α1 (1:250, cat# NBP1–30054, Novous Biologicals). The corresponding secondary antibodies used in the study were conjugated with AlexaFluor 488/594 (Invitrogen, CA).

Supporting Methods

Other methods, including liver perfusion, isolation of hepatocytes and HpSCs, phenotypic characterization of cells, ELISA, Western blot analysis, TUNEL assay, FISH, identification of SAM, liver function tests, reverse transcriptase polymerase chain reaction, primer design, and scanning electron microscopy are described.

Statistics

Results of multiple experiments were reported as mean ± SEM. Student's *t* test was carried out to calculate the significance between the means of both groups and $p < .05$ was considered as significant. All analyses were carried out using Graph pad Prism software, Version 5.02.

RESULTS

CD45 Cell Therapy Facilitates Regression of Fibrosis

The scheme for induction and maintenance of fibrotic conditions in mouse liver and transplantation of cells are shown in Figure 1A. A substantial regression of fibrosis was noticed in Tx_{CD45} group when compared with ShC and Tx_{MSC} groups, as determined by decline of the Metavir score from 3 to 1, and 70% CPA reduction within 30 days of transplantation (Fig. 1A–1C). In Tx_{MSC} group, the fibrosis too was significantly regressed, but at a much lower extent than Tx_{CD45} group. During fibrosis, HpSCs are activated to myofibroblasts and express α-SMA, most prominently along the septae. The α-SMA area was significantly reduced in Tx_{CD45} group but not in Tx_{MSC} when compared with the ShC group (Fig. 1A, 1D). Instead, a fraction (>20%) of engrafted cells in Tx_{MSC} group differentiated into myofibroblasts at they expressed both α-SMA and eGFP (4.5 ± 0.35 cells/field, ×600), which were completely absent in Tx_{CD45} group (Fig. 1E). Since, the regression of fibrosis was more prominently observed in Tx_{CD45} group, we further examined the resolution of fibrotic septae in liver sections by SEM. No fibrous collagen septae were seen in the healthy control samples. Interestingly, portal-to-portal septae that were observed in ShC were almost regressed after transplantation of CD45 cells (Fig. 1F). F1

In mouse BM, approximately 15% of CD45 cells are monocytes, the physiological precursors of macrophages. We propose that the monocytes present in the donor cells were converted into active macrophages in a fibrotic liver milieu and secreted more *MMPs* for the degradation of fibrillar collagen and elastin. Gene expression analyses showed significantly higher levels of *MMPs* in Tx_{CD45} group as compared to ShC group, whereas in the Tx_{MSC} only MMP-12 genes were enhanced (Fig. 2A). To validate the fibrolytic effect of CD45 cells and to decipher any immunosuppressive role of MSCs in this fibrolysis process, a cotransplantation experiment was conducted. It was revealed that the regression of fibrosis was significantly inhibited by the presence of MSCs, as shown by picrosirius red staining and CPA evaluation (Fig. 2B). We anticipate that cotransplantation prevented the accumulation of CD45 cells-derived macrophages near the fibrotic scar as compared to Tx_{CD45} group. This was confirmed by counting the number of MMP-13 expressing infiltrating cells adjacent to the scar (Fig. 2C). We expressed cell number in two ways—per field and unit fibrotic area basis. The purpose of showing MMP-13 expressing cell number in unit fibrotic area was that we analyzed liver after 30 days of transplantation, and in Tx_{CD45} group there was significant reduction of scar and so the total number of MMP-13 expressing cells per field. Morphometric analysis suggested that the average number of MMP-13 expressing macrophages in unit fibrotic area was reduced to one-third by the presence of MSCs as compared to CD45 cells alone (Fig. 2C, bar diagram). The above results show that in profibrotic condition, transplantation of CD45 cells improved liver fibrosis by providing more SAM than MSCs. F2

ID: parasuramank Time: 12:52 I Path: //chenas03/Cenpro/ApplicationFiles/Journals/Wiley/STEM/Vol00000/150206/Comp/APPFile/JW-STEM150206

J_ID: STEM Customer A_ID: STEM2210 Cadmus Art: STEM2210 Ed. Ref. No.: 15-0505.R1 Date: 24-September-15 Stage: Page: 4

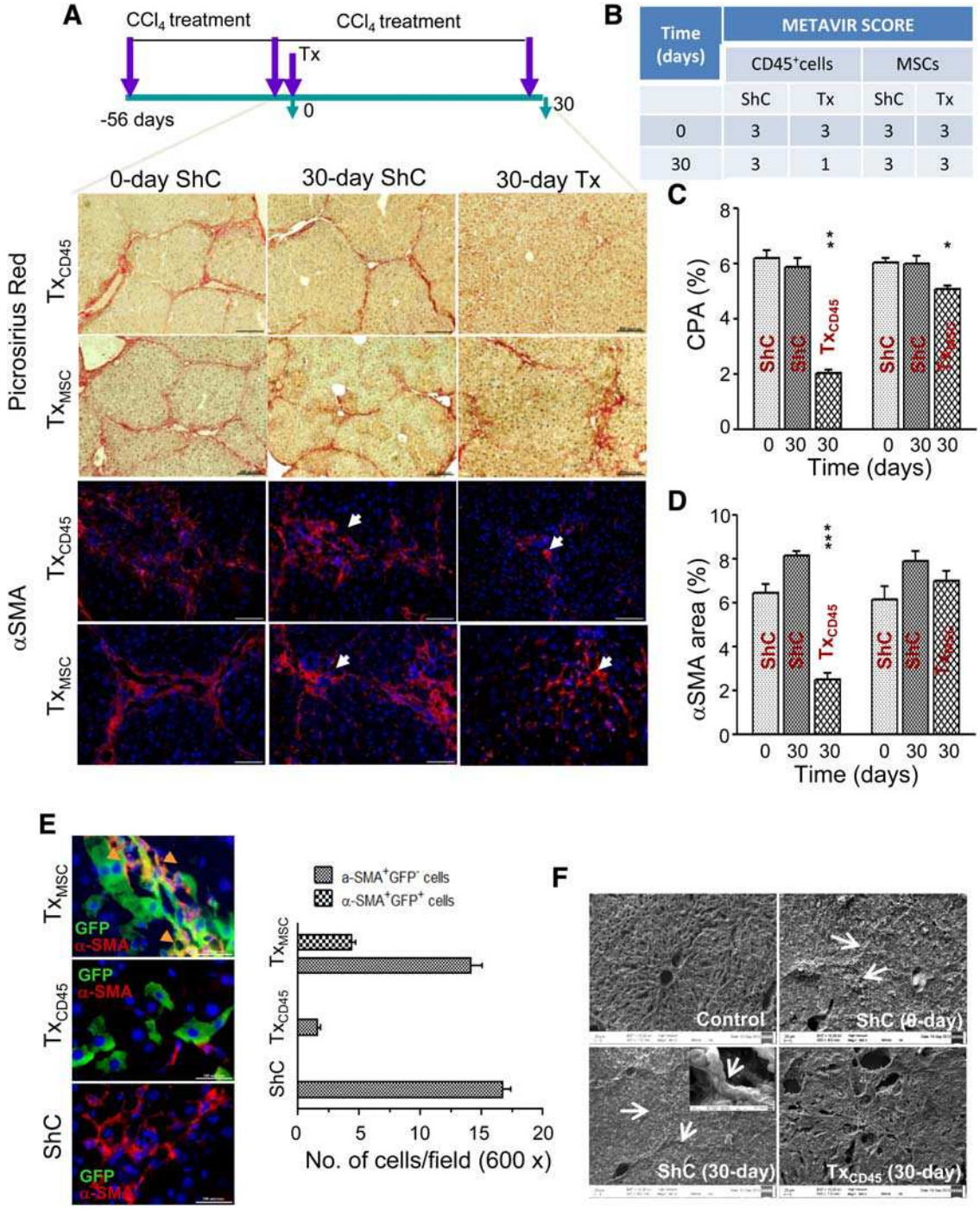

Figure 1. Therapeutic effect of CD45 cells/MSCs in fibrotic liver. **(A):** Plan of experiments and representative micrographs of liver sections are shown. CCl_4 administration was continued till the end of the experiment. Collagen was stained with picrosirus red and activation of stellate cells was assessed by α-SMA expression. Scale bar = 200 μm (×100) and 400 μm (×200). **(B):** Metavir score of fibrosis. Early resolution of fibrosis was seen in Tx_{CD45} group. **(C):** Collagen proportionate area. Percentage picrosirus red stained area was determined by Image J software from "A." Collagen synthesis in Tx_{CD45} group was significantly reduced as compared to ShC and Tx_{MSC} groups. **(D):** α-SMA area. Percentage α-SMA antigen expressing area was determined by Image J software. α-SMA area in Tx_{CD45} group was significantly reduced as compared to ShC and Tx_{MSC} groups. **(E):** Myfibroblastic differentiation of donor cells. Representative images show some eGFP-expressing donor MSCs also express α-SMA (orange arrows, top image), eGFP-expressing donor CD45 cells do not express α-SMA (middle image), and no eGFP expressing cells are present in ShC, but HpSCs are stained with α-SMA (bottom image). Scale bar = 50 μm (×600). Morphometric analysis based on 20 fields/mice is shown in the bar diagram. **(F):** Scanning electron micrographs. Representative figures show collagen septa (white arrows) in ShC liver, but not in the Tx_{CD45} mice. Magnification: ×500; inset shows highly magnified image (×30,650). Each analysis was based on biological replicates of three to six mice in each time point. *, < .05; **, < .01; ***, < .001. Abbreviations: GFP, green fluorescence protein; MSC, mesenchymal stem cell.

COLOR

ID: parasuramank Time: 12:52 I Path: //chenas03/Cenpro/ApplicationFiles/Journals/Wiley/STEM/Vol00000/150206/Comp/APPFile/JW-STEM150206

J_ID: STEM Customer A_ID: STEM2210 Cadmus Art: STEM2210 Ed. Ref. No.: 15-0505.R1 Date: 24-September-15 Stage: Page: 5

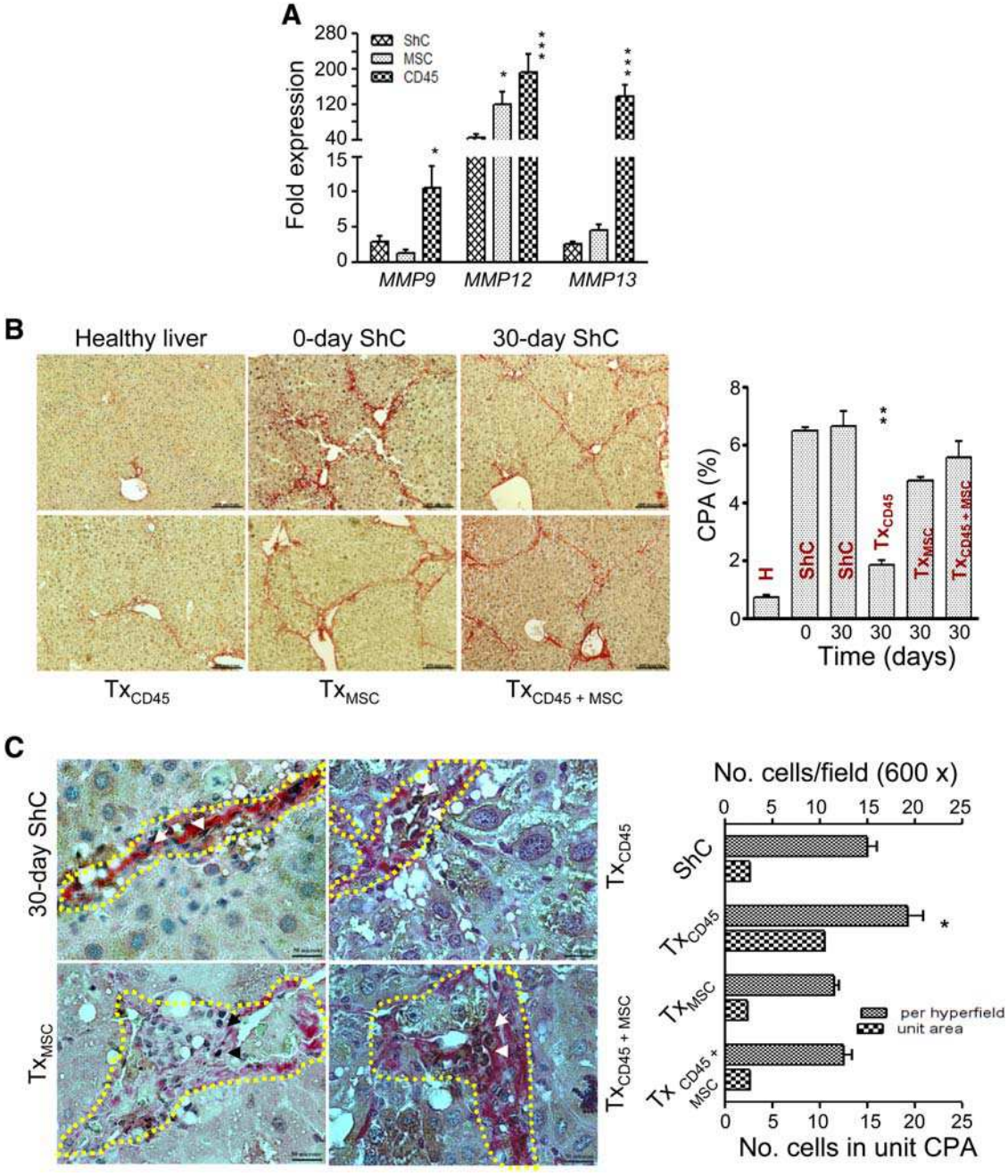

Figure 2. Effect of MSCs on fibrolytic activity of donor CD45 cells. **(A):** Comparative *MMP-9/12/13* gene expression after 30 days of transplantation. Real-time RT-PCR analyses show significantly high transcript levels of *MMP-9* and *−13* in Tx_{CD45} than ShC and Tx_{MSC} groups. **(B):** CPA. Micrographs of liver sections suggest cotransplantation of MSCs with CD45 cells results in suppression of fibrolytic effect of CD45 cells. CPA in Tx_{CD45} group was significantly low as compared to ShC, Tx_{MSC}, and $Tx_{CD45+MSC}$ groups. Scale bar = 200 μm (×100). **(C):** Accumulation of MMP-13 expressing cells near scar. Micrographs suggest cotransplantation of MSCs with CD45 cells do not resolute scar as compared to ShC, rather suppress resolution process. Morphometric analysis of the number of SAM (brown color stained) per field is based on average of 30–45 fields in multiple mice. The number of SAM is also converted into unit CPA basis. In each field, the counting of SAM was confined within collagen deposited zone (yellow color marked). The number of SAM is found to be much higher in case of Tx_{CD45} groups. Scale bar = 50 μm (×600). Each analysis was based on biological replicates of 3 mice. *, < .05; **, < .01; ***, < .001. Abbreviations: CPA, collagen proportionate area; MSC, mesenchymal stem cell.

C O L O R

CD45-CM Inactivates aHpSCs Whereas MSC-CM Induces Their Myofibroblastic Differentiation in Culture

It was clear from in vivo studies that among the two cell types, CD45 was superior in resolving the fibrosis. To decipher the molecular mechanisms by which CD45 cells or MSCs resolve fibrosis, we targeted HpSCs as their myofibroblastic differentiation leads to scar formation and their inactivation and/or apoptosis regress fibrosis. Initially, we performed contact and noncontact based coculture experiments using CD45 cells and HpSCs. It is known that HpSCs on activation differentiate into myofibroblasts, reduce retinoid bodies, and express α-SMA. The

ID: parasuramank Time: 12:54 I Path: //chenas03/Cenpro/ApplicationFiles/Journals/Wiley/STEM/Vol00000/150206/Comp/APPFile/JW-STEM150206

J_ID: STEM Customer A_ID: STEM2210 Cadmus Art: STEM2210 Ed. Ref. No.: 15-0505.R1 Date: 24-September-15 Stage: Page: 6

HpSCs, isolated from 8 weeks CCl_4-treated fibrotic liver, were cultured in the presence of CD45 cells (with/without contact) for 120 hours. The culture resulted in inactivation of aHpSCs as marked by the loss of α-SMA expression and gain of retinoid bodies in some cells (Supporting Information Fig. SF3). In control cultures, the activation of HpSCs was maintained till the end of the experiments. Cumulative scoring of α-SMA$^+$ cells in five independent experiments showed that the majority of the aHpSCs were inactivated in both contact and noncontact culture experiments.

Knowing that direct cell-to-cell contact is not essential for inactivation of aHpSCs, we then compared the relative antifibrotic potential of the conditioned media (CM). As the transplantation of MSCs showed a minor change in fibrosis, we thought that MSCs supported the myofibroblastic differentiation of HpSCs. To examine that, we separately cultured isolated HpSCs in the presence of 1:1 diluted CD45-CM or MSC-CM. The representative images show MSC-CM-induced complete myofibroblastic differentiation, as both collagen-1α and α-SMA synthesis were increased than in the control group, and cells attained a typical flat-spread morphology. Conversely, deactivation and reduction of cell number were noticed in the presence of CD45-CM when compared with control group and MSC-CM (Fig. 3A). Cumulative scoring of the results indicated a steep drop of α-SMA$^+$ cells number when cultured in CD45-CM (Fig. 3B, bar diagram). Interestingly, Wharton jelly MSC-CM also induced a myofibroblastic differentiation of HpSCs (Supporting Information Fig. SF4). F3

Next, we compared overall proliferation of HpSCs in the presence of conditioned media by MTT assay. The results showed that MSC-CM induced twofold more proliferation as compared to control within 48 hours of culture, whereas the proliferation was inhibited by CD45-CM (Fig. 3B). Further analysis confirmed that a few activated and normal HpSCs expressed nuclear proliferating antigen (Ki67). Quantitative analyses of cells expressing α-SMA and Ki67 indicate that MSC-CM supported the proliferation of aHpSCs, whereas CD45-CM induced the proliferation of normal HpSCs (Fig. 3C).

We deciphered the molecular mechanism to confirm the fibrogenic potential of MSCs. A high level of TGFβ, an inducer of fibrosis, in MSC-CM indicated its potential role in the myofibroblastic differentiation of HpSCs (Fig. 3D). In order to determine whether this secreted TGFβ has any paracrine role, we cultured HpSCs in control and conditioned media, but in absence or presence of a TGFβ receptor kinase inhibitor. It was observed that, like in earlier experiments, both control medium and MSC-CM induced a myofibroblastic differentiation of HpSCs, as they expressed α-SMA and collagen-1α; however, such cellular changes were significantly barred in the presence of inhibitor (Fig. 3E, Supporting Information Fig. SF5). In percentile, we could not found much difference in activated HpSCs between control medium and MSC-CM as in both cases cells were isolated from 8th week fibrotic liver (Fig. 3E, bar diagram), but higher expressions of both α-SMA and collagen-1α were observed in case of MSC-CM-treated cells (Supporting Information Fig. SF5). Since CD45-CM did not show any myofibroblastic differentiation, no inhibitory effect of SB-431542 was noticed (Fig. 3E). These results confirmed the role of MSC-secreted TGFβ for myofibroblastic differentiation of HpSCs, which was not discernible in case of CD45-CM.

CD45-CM Induces Apoptosis, Whereas MSC-CM Suppresses Apoptotic Death in aHpSCs

The growth inhibitory effect of CD45-CM on aHpSCs was confirmed by gene expression analysis, in which proapoptotic (*Bad*) and cell cycle inhibitor (*p27*) genes were significantly increased in CD45-CM-treated cells (Supporting Information Fig. SF6). The activation of *Bad* and *p27* genes in this case may lead to further sensitization of cells toward apoptosis. To identify the presence of death ligands in CD45-CM/MSC-CM, first their gene expressions (*FasL*, *TNF*α, and *TRAIL*) were compared in the cells. Also, we analyzed gene expressions for platelet-derived growth factor (PDGF), a potent mitogen for aHpSCs and IFNγ, an inhibitor of TFGβ pathway in both cell types. The results confirmed the prominent expression of "death ligands" genes in CD45 cells, which were minimally expressed in MSCs (Fig. 4A). Different forms of *PDGF* genes were expressed both in CD45 and MSCs, whereas *IFN*γ was solely present in CD45 cells (Fig. 4A). The FasL was present in much higher amount in CD45-CM, which led to build our hypothesis that enhancement of apoptotic death in aHpSCs was due to this secreted factor (Fig. 4B). Later, a bioneutralization assay of FasL in CD45-CM confirmed the apoptotic/growth inhibitory effect, as proliferation of HpSCs was partly restored (Fig. 4C) and cells moderately expressed the differentiation antigen (α-SMA) in a FasL neutralized culture medium as compared to normal CD45-CM (Fig. 4D). F4

To confirm that FasL induces apoptosis in aHpSCs, we conducted caspase-3/7 activity assay after 20 hours of preincubation with conditioned media. The results showed an additive effect of CD45-CM on caspase-3/7 activity, over and above the one that was observed in the control group and MSC-CM (Fig. 4E). The antiproliferative and apoptotic effect of CD45-CM on aHpSCs were also evidenced by nuclear condensation, which were absent in case of MSC-CM (Fig. 3B). To know whether CD45 cell transplantation can induce apoptosis in HpSCs, we analyzed desmin$^+$ cells in liver sections for TUNEL reaction. The results suggested that a fraction of HpSCs still underwent apoptosis even after 30 days of transplantation (Supporting Information Fig. SF7).

Since apoptosis of cells in the presence of MSC-CM was comparable to that of control medium and much lower than CD45-CM, we measured insulin-like growth factor-1 (IGF-1) titer, a potent antiapoptotic factor of aHpSCs, in conditioned media. It was found that approximately 10-fold more IGF-1 was present in MSC-CM as compared to control medium or CD45-CM (Fig. 4F). Summarizing the above results, CD45-CM consists of proapoptotic factors, which are present in suboptimal level in MSC-CM to make any effect on aHpSCs. Conversely, MSC-CM contains significantly higher level of antiapoptotic factor than CD45-CM, so rescued cells from undergoing apoptosis.

CD45 Cells Transplantation Leads to Improvement of Liver Function

Liver function is compromised in the case of chronic injury. As fibrosis was significantly suppressed due to transplantation of CD45 cells, we expected a corresponding improvement of liver function in these mice. Liver function tests have shown that CD45 cell therapy resulted in the decline of alanine transaminase

ID: parasuramank Time: 12:55 I Path: //chenas03/Cenpro/ApplicationFiles/Journals/Wiley/STEM/Vol00000/150206/Comp/APPFile/JW-STEM150206

J_ID: STEM Customer A_ID: STEM2210 Cadmus Art: STEM2210 Ed. Ref. No.: 15-0505.R1 Date: 24-September-15 Stage: Page: 7

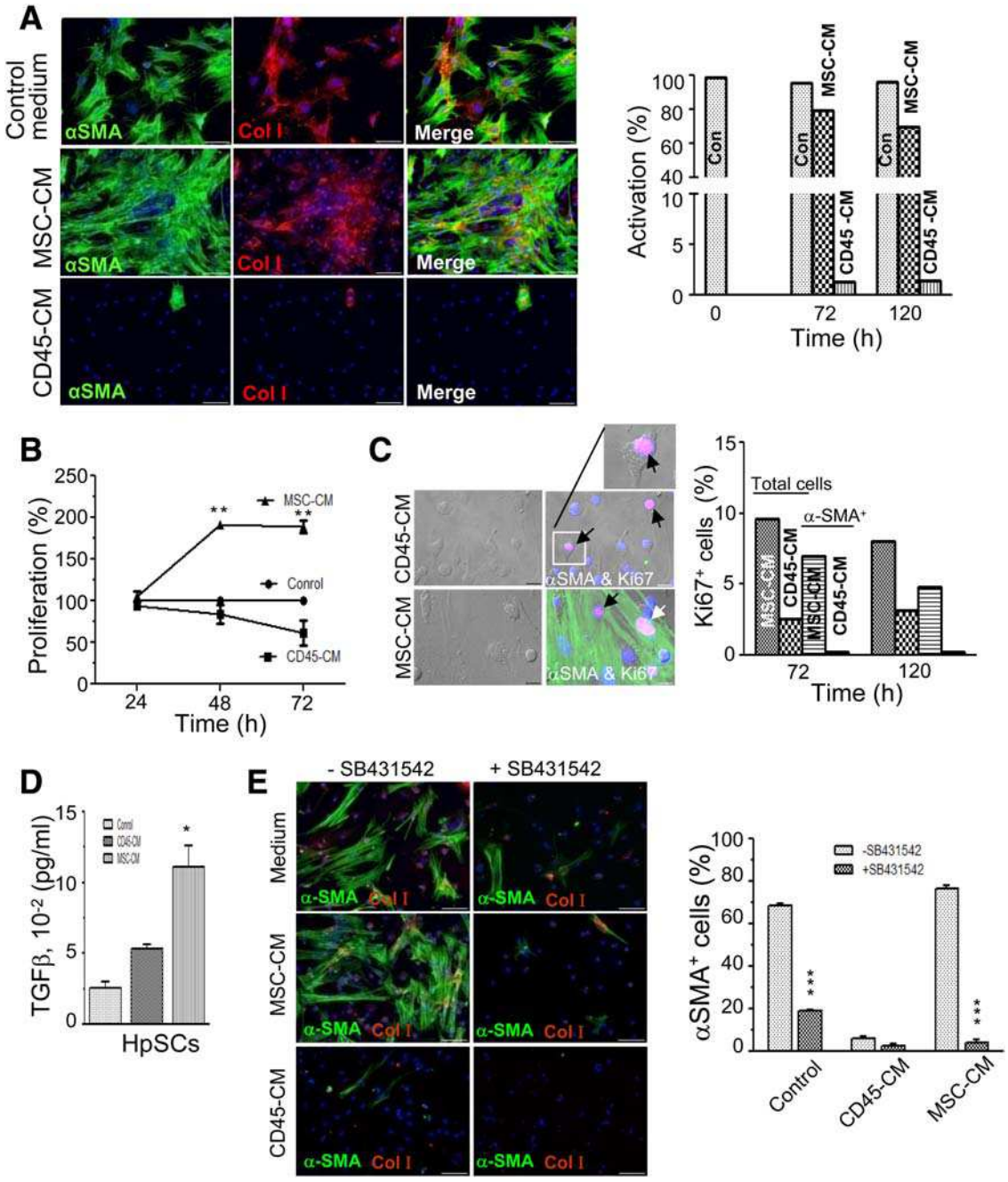

Figure 3. Effects of CD45-CM on inactivation and MSC-CM on activation of HpSCs in culture. **(A):** Inactivation of aHpSCs in 1:1 diluted CD45- or MSC-CM. Cells, cultured for 72 and 120 hours in three different media, were costained for α-SMA and collagen-1α1. Representative images show the expression of α-SMA and collagen-1α by aHpSCs. The expressions of these activation markers were suppressed in the presence of CD45-CM. Bar diagram shows (cumulative 500 cells/experiment) CD45-CM was more potent for inactivating myofibroblasts than that of MSC-CM ($n = 3$). Scale bar = 400 μm (×200). **(B):** Proliferation of aHpSCs in 1:1 diluted conditioned media. Fifty thousand cells were cultured in 48-well plate in triplicate wells; proliferation was assessed by MTT assay. At each time interval, relative proliferation was determined with respect to the control wells (normal medium) ($n = 4$). **(C):** Proliferation of aHpSCs in 1:1 diluted conditioned media. Nuclear antigen Ki67 was expressed in two types of HpSCs (α-SMA$^+$: white arrow and α-SMA$^-$: black arrows). Both types of cells were apparently hepatic stellate cells. Bar diagram shows (cumulative 500 cells/experiment) MSC-CM contributed toward more proliferation of aHpSCs ($n = 3$). Scale bar = 50 μm (×600). **(D):** Concentrations of TGFβ in control and 1:1 diluted conditioned media were determined by ELISA (BD Biosciences, San Diego, CA) ($n = 4$). **(E):** Expression of α-SMA and collagen-1α in aHpSCs after 72 hours of culture in 1:1 diluted conditioned or normal media in absence or presence of 50 μM SB-431542 inhibitor. Representative images show that, in the presence of inhibitor, the expressions of these markers of myofibroblastic differentiation are completely abrogated in cases of control and MSC-CM media. Scale bar = 400 μm (×200), $n = 3$. The results of experiment "E" were quantitatively analyzed and presented in bar diagram by counting α-SMA expressing cells from three experiments. *, < .05; **, < .01; ***, < .001. "*n*" is the number of experiments. Abbreviations: CM, conditioned medium; HpSCs, hepatic stellate cells; MSC, mesenchymal stem cell.

COLOR

ID: parasuramank Time: 12:55 I Path: //chenas03/Cenpro/ApplicationFiles/Journals/Wiley/STEM/Vol00000/150206/Comp/APPFile/JW-STEM150206

J_ID: STEM Customer A_ID: STEM2210 Cadmus Art: STEM2210 Ed. Ref. No.: 15-0505.R1 Date: 24-September-15 Stage: Page: 8

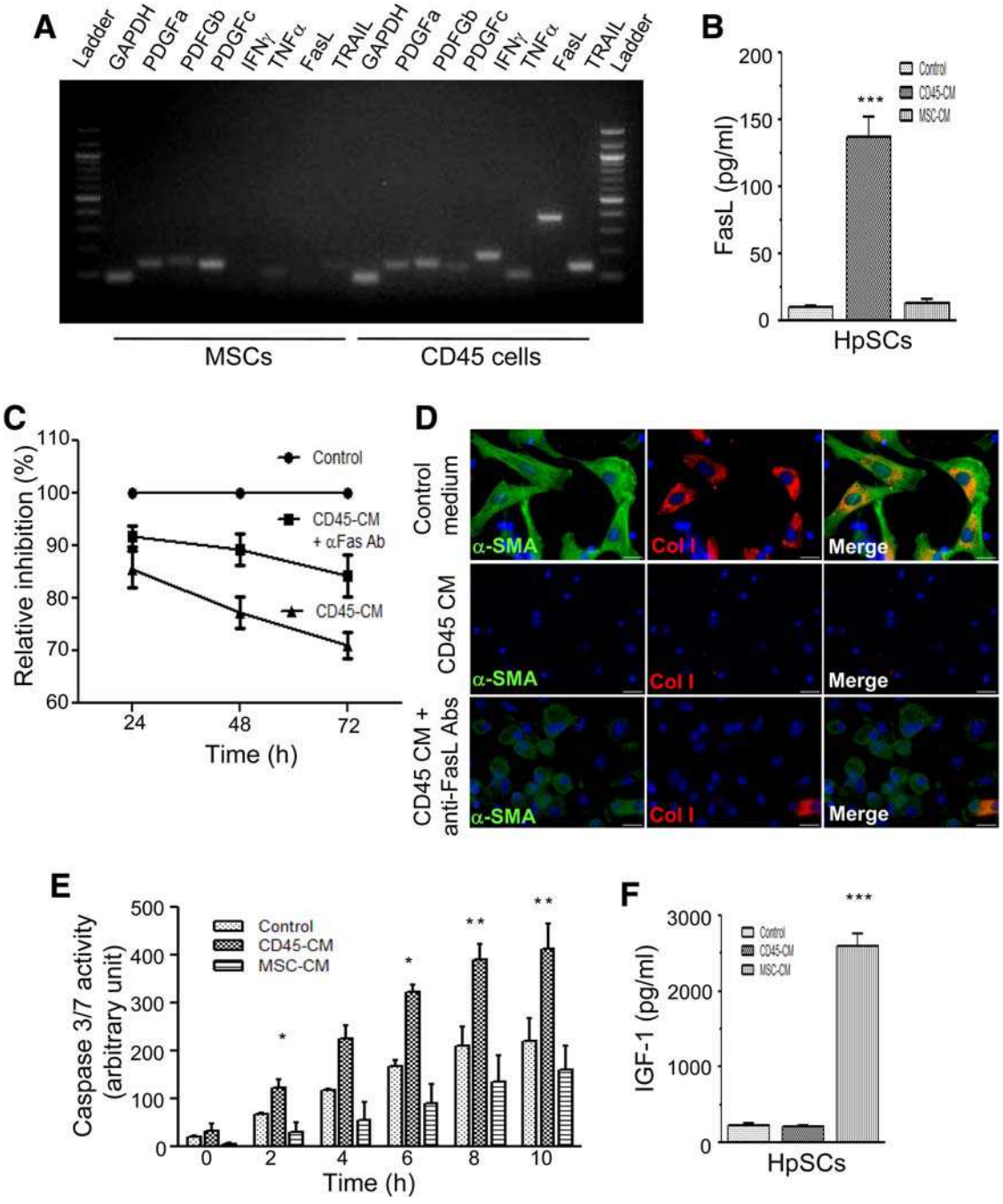

C O L O R

Figure 4. Effect of FasL and TGFβ on growth inhibition and differentiation of HpSCs, respectively. **(A):** RT-PCR analyses of different cytokine genes in MSCs and CD45 cells that are responsible for apoptosis and proliferation of HpSCs ($n = 4$). **(B):** Concentrations of FasL in control and 1:1 diluted conditioned media were determined by ELISA (Boster Biological, Pvt. Ltd.) ($n = 4$). **(C):** Bioneutralization assay for FasL. Fifty thousand cells were cultured in 48-well plate in triplicate wells for 24, 48, and 72 hours in the presence of control medium and 1:1 diluted CD45-CM (preincubated with anti-FasL antibody, R&D Systems). Growth inhibition was assessed by MTT assay. At each time interval, relative inhibition was determined with respect to the control wells ($n = 3$). **(D):** Inactivation of aHpSCs in 1:1 diluted CD45-CM (absence/presence of anti-FasL antibody). After 72 hours of culture, cells were stained for α-SMA and collagen-1α. Representative images show the absence of α-SMA and collagen-1α expression in CD45-CM, whereas α-SMA is partially expressed in FasL neutralized media. Scale bar = 50 μm (×600). **(E):** Apoptosis of aHpSCs. Cells were cultured in the presence of normal and CM, and then Caspase-3/7 activities (Apo-one Homogeneous Caspase-3/7 Assay kit, Promega Corporation) were assayed at different times ($n = 3$). **(F):** Concentrations of IGF-1 in control and 1:1 diluted conditioned media were determined by ELISA (Peprotech Asia, Israel) ($n = 4$). *, $< .05$; ***, $< .001$. "n" is the number of experiments. Abbreviations: CM, conditioned medium; HpSCs, hepatic stellate cells; MSC, mesenchymal stem cell.

AQ7

and improvement of albumin levels in sera as compared to ShC mice (Fig. 5A, 5B). Conversely, the transplantation of MSCs did not show any functional improvement of the liver with respect to these parameters (Fig. 5A, 5B). The above results suggested that CD45 cells were involved in the repair of liver more efficiently that MSCs.

F5

ID: parasuramank Time: 12:55 I Path: //chenas03/Cenpro/ApplicationFiles/Journals/Wiley/STEM/Vol00000/150206/Comp/APPFile/JW-STEM150206

J_ID: STEM Customer A_ID: STEM2210 Cadmus Art: STEM2210 Ed. Ref. No.: 15-0505.R1 Date: 24-September-15 Stage: Page: 9

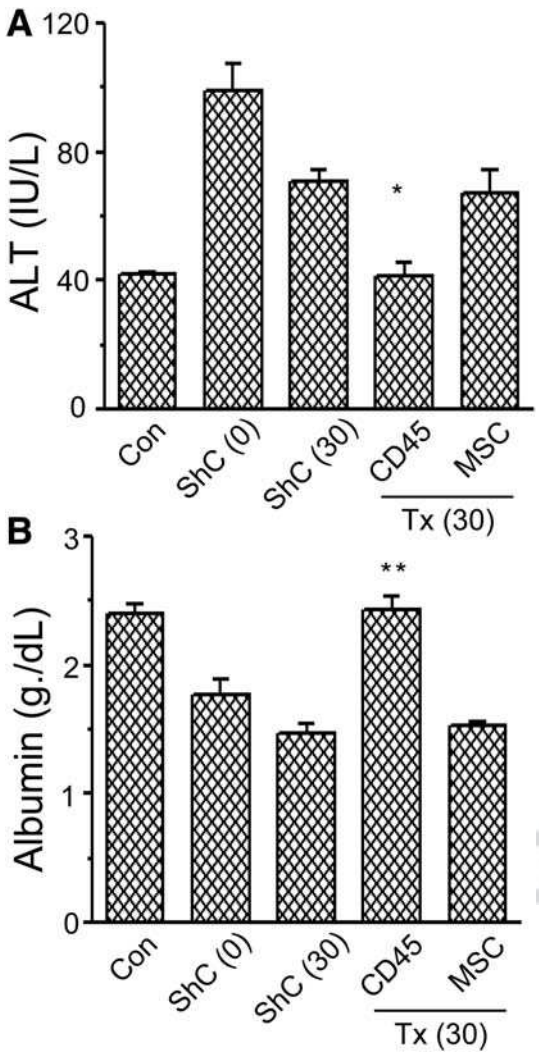

Figure 5. Functional recovery of liver. **(A):** After 8 weeks of CCl_4 treatment, mice were divided into three groups. ShC group received PBS and other two groups received CD45 cells or MSCs as per schedule. CCl_4 treatment was continued in these mice for another 30 days. Sera ALT of normal control, ShC, and transplanted mice were analyzed and compared. **(B):** In above experiments, sera albumin levels were analyzed and compared. ALT and albumin levels were determined using commercially available kits (Transasia Biomedicals, India). Experiments were conducted in three batches consisting of 15 sera samples. *, $<.05$; **, $<.01$. Abbreviations: ALT, alanine transaminase; MSC, mesenchymal stem cell.

BM-CD45 Cells Contribute to Liver Regeneration

As liver function improvement was only observed in Tx_{CD45} group, we further analyzed the engraftment and contribution of donor cells in liver regeneration. Photomicrographs of liver sections suggested the engraftment of donor CD45 cells in the fibrotic liver and their retention even after 60 days of transplantation. Interestingly, the engrafted donor cells changed their phenotype and expressed hepatic markers like albumin and CK18 (Fig. 6A, right panel). The sham control liver sections did not react with isotype control sera or an eGFP antibody, indicating the specificity of the staining procedure (Fig. 6A, left panel). The percentage GFP^+, GFP^+Alb^+, and GFP^+CK18^+ cells per field were determined by morphometric analysis of images (Supporting Information Fig. SF8). The results revealed that almost 15% hepatocytes of the recipient liver were donor-originated (Fig. 6B). The IHC result was validated by semiquantitative Western blot analysis in which we enumerated $16.85\% \pm 2.52\%$ ($n = 3$) liver cells were eGFP expressing (Fig. 6C). The difference in results could be attributed to the specificity of the antibodies used in two readouts, independent assay methods, and uneven distribution of donor-derived cells in liver. Besides hepatic phenotype, a few BM-derived endothelial cells and Kupffer cells were also detected (Supporting Information Fig. SF9). Mice with Tx_{MSC} group also showed the presence of donor cell-derived hepatocytes (data not shown).

To know whether host or donor-derived hepatocytes can proliferate following transplantation of CD45 cells, liver sections were costained for Ki67 and eGFP. A few host and donor-marked cells, morphologically resembling hepatocytes, expressed nuclear Ki67 antigen (Fig. 6C, Supporting Information Fig. SF10). Further analysis revealed that relatively more $eGFP^+$ hepatocytes expressed Ki67 as compared to host hepatocytes, indicating that donor-derived cells proliferated during liver regeneration. To examine whether transplantation of cells leads to the activation of hepatic progenitor cells (HPCs), we stained 30 days liver sections with CK19 and Ki67. The results clearly indicated that in Tx_{CD45} group there was significantly ($p < .001$) high level of ductular reactions, marked by CK19 staining, as compared to ShC and Tx_{MSC} group (Fig. 6D, Supporting Information Fig. SF11). Despite DR response was observed in Tx_{CD45} group, no proliferating HPCs were detected.

To examine the heterogeneity of sex chromosome, if any, in eGFP-expressing hepatic cells we conducted an X,Y FISH cytogenetic analysis of the sorted cells after 2 months of transplantation (Fig. 6E, Supporting Information Fig. SF12). We analyzed 1,133 nuclei of sorted $eGFP^+$ hepatocytes, of which 93.65% of the cells were a mixture of diploid, tetraploid, and hexaploid X-chromosome (XX, XXXX, XXXXXX) containing. Approximately 4.75% of the cells possessed both X- and Y-chromosome (XXXY, XXY, XY), whereas balance of 1.58% was aneuploid (XXX, XXXXX). Interestingly, the donor-derived hepatic cells lost CD45 antigen (Fig. 6F). Overall, these results suggested that most of the donor cells-derived eGFP-expressing hepatocytes do not contain host chromosome, undergo partial reprogramming and participate in liver regeneration process.

DISCUSSION

In CLI, activation of HpSCs leads to liver fibrosis as they secrete excess fibrillar collagen, elastin, and other matrix proteins. In the past 10 years, many clinical trials have been pursued for the treatment of cirrhotic and genetic liver diseases by transplanting crude BM cells or MSCs. In most of these cases no adverse incidence was reported, while slight improvements of clinical parameters were registered [6, 22]. Since liver fibrosis/cirrhosis is associated with chronic inflammation, there is widespread enthusiasm for using MSCs as immunomodulators [23]. However, many contradicting reports have been published on the therapeutic potential of MSCs, which seem to be attributed to the type of experimental model, MSCs' phenotype, and cells' dosage [24]. In this report, we have demonstrated that BM-CD45 cells were superior to MSCs in the therapeutic intervention of liver fibrosis and dissected the mechanisms.

ID: parasuramank Time: 12:56 I Path: //chenas03/Cenpro/ApplicationFiles/Journals/Wiley/STEM/Vol00000/150206/Comp/APPFile/JW-STEM150206

J_ID: STEM Customer A_ID: STEM2210 Cadmus Art: STEM2210 Ed. Ref. No.: 15-0505.R1 Date: 24-September-15 Stage: Page: 10

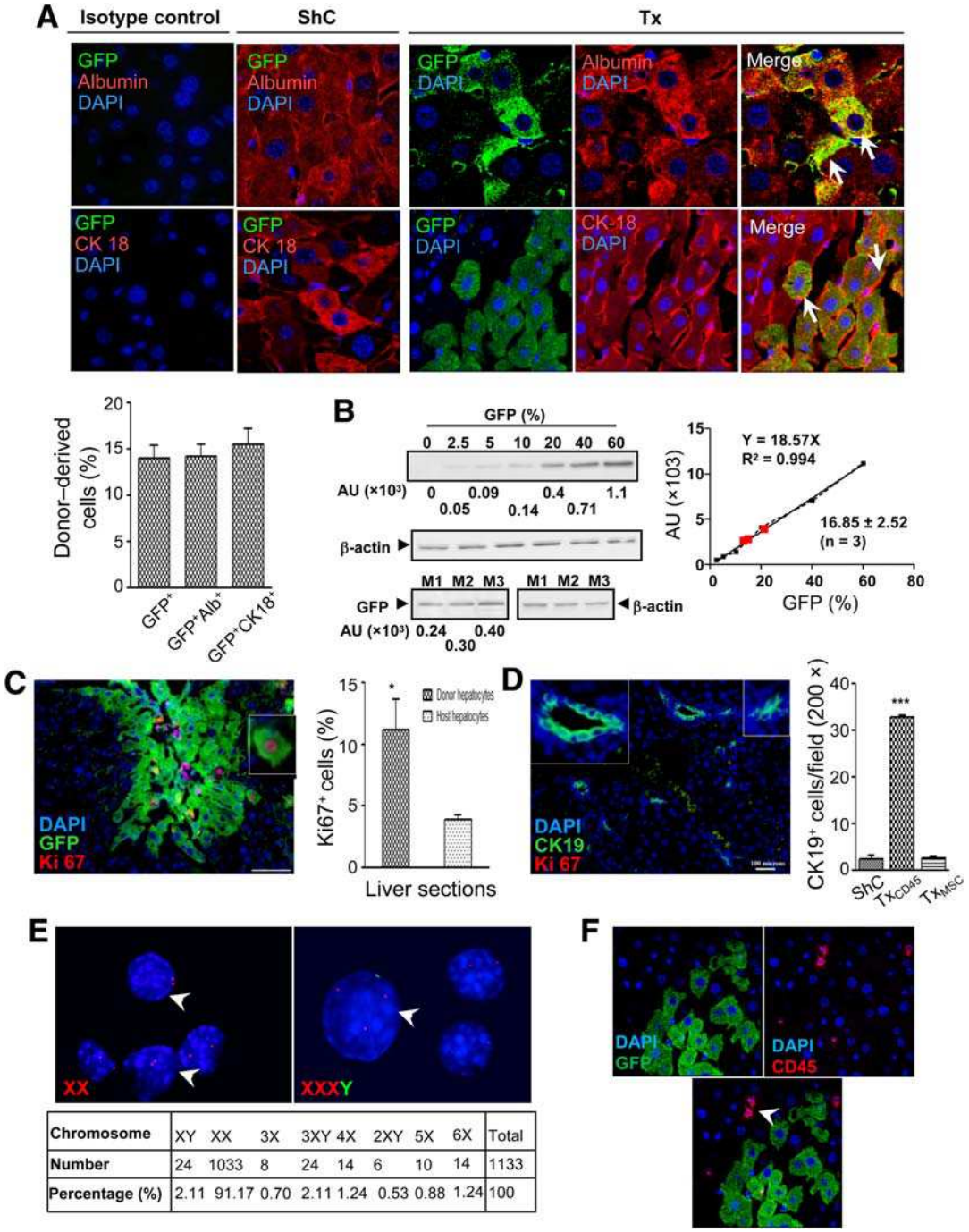

Chromosome	XY	XX	3X	3XY	4X	2XY	5X	6X	Total
Number	24	1033	8	24	14	6	10	14	1133
Percentage (%)	2.11	91.17	0.70	2.11	1.24	0.53	0.88	1.24	100

COLOR

Figure 6. Phenotype conversion of engrafted CD45 cells and cytogenetic analysis. **(A):** Liver sections (after 60 days of transplantation) show that bone marrow (BM)-derived cells express albumin (right top panel) and CK18 (right bottom panel). Staining was specific as isotype control sera did not show any reactions (left panel). Magnification = ×600. Bar diagram shows quantitative analysis of cellular phenotype in BM-derived cells. Calculation was made on the basis of morphometric analyses from nonoverlapping 30 fields/mouse (×200) of representative images (Supporting Information Fig. SF8) after 60 days of transplantation. **(B):** Semiquantitative Western blot analysis of eGFP protein. eGFP protein bands of calibrating and test (recipient mouse: M1, M2, and M3) samples, and corresponding loading controls (β-actin) bands are shown. Calibration curve in AU versus percentage eGFP-expressing cells, and values of unknown samples are shown. **(C):** Expression of Ki67 nuclear antigen in hepatocytes. Representative image shows few hepatocyte nuclei (white arrow: host cell, red arrow: donor cells) express Ki67 antigen after 30 days of transplantation. Scale bar = 400 μm (×200), $n = 3$. Morphometric analysis based on 15 fields/mouse is shown in the bar diagram. **(D):** Activation of ductular reactions. Representative image (inset) shows few ductular reactions marked by CK19 staining after 30 days of transplantation. Scale bar = 100 μm (×200), $n = 3$. Morphometric analysis (comparative) based on 20 fields/mouse is shown in the bar diagram. **(E):** FISH of X, Y chromosome. The nuclei of representative unfused (XX, top image) and highly selected fused (XXXY, bottom image) donor-derived hepatocytes are shown (white arrow). Percentile distributions of fused and unfused cells are shown in the table. Magnification = ×1,000. **(F):** Expression of CD45 antigen. Morphologically distinct donor-derived hepatic cells do not express CD45, but non-mesenchymal cells (white arrow) express the same antigen. Magnification: ×600 ($n = 3$). "n" is the number of animals. *, < .05; ***, < .001. Abbreviations: AU, absorption unit; DAPI, 4′,6-diamidino-2-phenylindole; GFP, green fluorescence protein.

ID: parasuramank Time: 12:56 I Path: //chenas03/Cenpro/ApplicationFiles/Journals/Wiley/STEM/Vol00000/150206/Comp/APPFile/JW-STEM150206

J_ID: STEM Customer A_ID: STEM2210 Cadmus Art: STEM2210 Ed. Ref. No.: 15-0505.R1 Date: 24-September-15 Stage: Page: 11

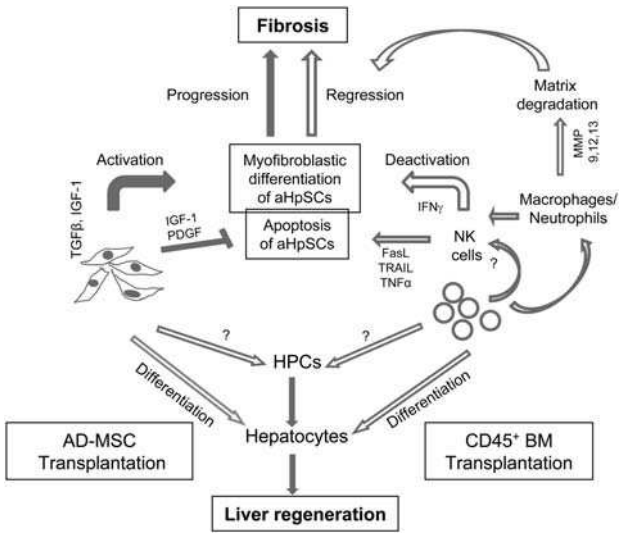

Figure 7. Proposed mechanisms of action of donor cells (CD45/MSC) on fibrotic liver. The immunomodulatory function of MSCs suppress inflammation to cirrhotic liver leading to lower fibrolytic effect of resident KCs and SAM. Furthermore, synthesis of TGFβ, IGF-1, PDGF, and so forth, by MSCs protect aHpSCs from apoptosis and allow their myofibroblastic differentiation and subsequent proliferation, which results in more collagen-1α synthesis leading to scar formation. MSCs can also take part in indirect (paracrine effect on HPCs) and direct (differentiation into hepatocytes) liver regeneration process. Crude CD45 cells is composed of hematopoietic stem cells and progenitor cells, they can also take part in indirect and direct liver regeneration process. Monocytes present in CD45 cells differentiate into active macrophages (SAM) in the liver milieu that together with neutrophils secrete large amount of MMP-9,12,13 for effective degradation of fibrotic scar. Conversely, death ligands (FasL, TRAIL, and TNFα) secreted by NK cells facilitate apoptotic death of aHpSCs and a potent inhibitor of TGFβ pathway (IFNγ) for preventing myofibroblastic differentiation. The overall effect of CD45 cells will be resolution of fibrosis, liver regeneration, and restoration of normal liver function, whereas MSCs suppress the resolution process (shown by cotransplantation experiments). Closed and open arrows show the potential action pathways of MSCs and CD45 cells, respectively. (?): Potential effector molecules are not studied in this report. Abbreviations: AD-MSCs, adipose-derived mesenchymal stem cells; BM, bone marrow; HPCs, hepatic progenitor cells; NK cells, natural killer cells; SAM, scar-associated macrophages.

Among all immune cells, macrophages are considered master regulators in the progression as well as the resolution of liver fibrosis. In fibrosis regression, the infiltrating macrophages adopt fibrolytic phenotypes to secrete MMP-9,12,13 for the degradation of excess ECM components [11, 15, 25]. We propose that the macrophage precursors, present in the donor CD45 cells, were converted into active fibrolytic macrophages (SAM) in a fibrotic liver milieu by the influence of macrophage-colony-stimulating factor (M-CSF) secreted by activated HpSCs [26]. This may accounted for the significantly higher levels of *MMP-9/12/13* in Tx_{CD45} group, leading to the degradation of scar and early recovery. MSC transplantation, conversely, suppressed the recruitment of these macrophages in fibrotic liver [9, 10] resulting in an incomplete degradation of scar. This observation was validated in our cotransplantation experiments as the degradation of scar due to CD45-derived macrophages was compromised and relatively low number of SAM were detected near the scar. It is important to mention here that MSC transplantation did not improve tissue level *MMP-9,13* gene expression, which are supposed to degrade collagen [27]. Our results emphatically conclude that in situ differentiated macrophages have the potential to dissolve fibrotic scar, and thus therapy using in vitro differentiated macrophages [16] would not be required. The increasing trend of *MMP-9,12* could also be due to the neutrophils present in the donor cells.

Interestingly, we observed that aHpSCs were eliminated or inactivated more efficiently after transplantation of CD45 cells as compared to MSCs. In response to inflammation, HpSCs are activated into myofibroblasts and proliferated by the action of TGFβ and PDGF, respectively, that are secreted by macrophages [11–13]. During regression of fibrosis, these aHpSCs are reduced in number by combination of deactivation and apoptosis [28]. The liver sections of the Tx_{CD45} group not only showed that the ECM components were efficiently degraded, but that the cells making these proteins were also declined in number. In vitro experiments showed that CD45-CM promotes apoptosis in aHpSCs. At the same time, a major fraction of them returned to the inactivated or quiescent state. Quiescent HpSCs possess retinoid bodies, which are eventually lost upon activation and differentiation. The presence of retinoid bodies in cultured HpSCs confirmed that they have departed from cell cycle or have never been activated. Apoptotic effect of CD45-CM to aHpSCs may be due to the action of death ligands present in the CM, which are potentially secreted by NK cells and proresolving/fibrolytic macrophages [11, 29–31]. We have confirmed the functions of FasL by a bioneutralization assay, although its contribution toward death was found to be low. Here, we only examined the role of FasL, it does not seclude TNFα− and TNF-related apoptosis inducing ligand (TRAIL) as apoptotic agents. Therefore, we propose the additive effect of all three factors in the enhancement of apoptotic death in aHpSCs.

Our in vivo results using MSCs were not in accord with the preclinical results on the regression of fibrosis, although we transplanted lower number of cells to avoid unwanted mortality [6]. Despite low dose of MSCs, cotransplantation experiment confirmed that this low number of cells were enough to reverse the antifibrotic effect of CD45 cells, transferred in the liver. In the rat model no improvement of fibrosis was reported following the transplantation of MSCs [32]. Surprisingly, we detected α-SMA expressing donor-derived cells only in the Tx_{MSC} group, as reported by others [18, 19, 33]. Furthermore, like other cells, MSCs are also known to secrete many factors, such as vascular endothelial growth factor, TGFβ, PDGF, and IGF-1 [34–37], which can protect aHpSCs from undergoing apoptosis, induce myofibroblastic differentiation, and proliferation. Our results support above notions, since we first observed high expression of α-SMA and collagen-1α in a culture of HpSCs in MSC-CM due to the activation of TGFβ pathway. Second, we have demonstrated overall proliferation and low apoptosis in these cells, possibly by the combined effect of PDGF and IGF-1 present in MSC-CM. In contrast, CD45-CM neither supported the myofibroblastic differentiation of HpSCs nor protected them from undergoing apoptosis, but, rather facilitated cellular death.

Activated liver resident NK/NKT cells were shown to possess strong antifibrotic activity in vivo, as they selectively kill early or senescence aHpSCs by secreting TRAIL/FasL and IFNγ [38]. Again, TGFβ attenuates NK cells cytotoxicity against aHpSCs

ID: parasuramank Time: 12:56 I Path: //chenas03/Cenpro/ApplicationFiles/Journals/Wiley/STEM/Vol00000/150206/Comp/APPFile/JW-STEM150206

J_ID: STEM Customer A_ID: STEM2210 Cadmus Art: STEM2210 Ed. Ref. No.: 15-0505.R1 Date: 24-September-15 Stage: Page: 12

[39]. Overall, above reports suggest that the NK cells' activation and the absence of TGFβ are two most favorable conditions for killing of aHpSCs. The myofibroblastic differentiation of HpSCs and their proliferation in the culture have raised questions against antifibrotic potential of MSCs, although TGFβ and PDGF are not exclusively synthesized by these cells in vivo. Here, we propose that immune-suppressive properties of MSCs attenuated the functions of NK cells, macrophages, and neutrophils, thereby compromised the regression of fibrosis [25, 26].

Postinjury liver is regenerated by activation and proliferation of hepatic progenitor cells [40]. Interestingly, CD45 cell transplantation showed the presence of massive DRs as compared to MSCs. In liver, DR sites are composed of HPCs; it has been shown that macrophages of BM cells are capable of inducing DRs in healthy mice liver through TWEAK signaling [41]. Although DRs were present, no proliferating HPCs were detected. We assume that HPCs proliferation is an early event in DRs, within few days of transplantation, which was probably ceased by the time of analysis. Here, we have shown, using two alternate methods, a high proportion of hepatic cells in the recipient liver that expressed donor eGFP marker. A large number of donor-derived hepatocytes were probably due to: (a) intrasplenic transplantation allowed better engraftment of CD45 cells in the liver as compared to their systemic delivery due to direct supply of cells to the hepatic plates via portal vein, and (b) high proliferation of donor-derived cells as compared to the host hepatocytes. We observed entrapment of donor cells in spleen at the beginning of infusion, which later mostly egress to the liver. Even though BM-derived hepatocytes were reported in the literature [42–45], the plasticity of BM stem cells had been questioned by many groups [46–48]. Earlier, by lineage tracking analysis of transgenic mice, it was revealed that hepatocyte-like cells are exclusively generated after ploidy reduction of the fusion heterokaryons of BM cells and host hepatocytes within 5–7 days of transplantation [49]. Furthermore, the ploidy reduction was found to be associated in part with the loss of both donor marker and host chromosome at the time of chromosomal segregation [49]. If in situ cell fusion is the only mechanism in formation of BM-derived hepatocytes, it was possible that in this study fusion hybrids were segregated much early, and thus very few of them were detected by FISH after 2 months of transplantation. Interestingly, the donor-originated hepatic cells underwent partial nuclear reprogramming as they lost the pan hematopoietic marker, CD45.

Conclusions

In summary, we have shown that BM-CD45 cell therapy improved structural and functional parameters in CCl_4-induced fibrotic liver, which was not clearly evidenced in case of MSCs. We envisaged CD45 cells in clusters of three important populations of functional relevance, (a) Lin^- cells and hematopoietic stem cells that are involved in liver regeneration and activating hepatic progenitor cells, (b) monocytes/macrophages and neutrophils that facilitate the degradation of fibrous scar and the death of myofibroblasts, and (c) NK cells that promote apoptotic death of myofibroblasts, as depicted in Figure 7. Here, we propose that MSC-mediated immune-suppression may be beneficial provided it is available at the beginning of the fibrosis. A highly efficient immune-suppressing system may adversely influences the fibrolysis process as the functions of resident and circulating fibrolytic cells are dampened. In clinical translation, CD45 cell therapy, rather than MSCs, is believed to be most appropriate as cells can be easily harvested and transfused, and no culture manipulation is required.

Acknowledgments

We are thankful to Dr. Vikash Kumar for supporting flow cytometry-based analysis. Last author is thankful to Department of Biotechnology, Government of India for generous support for the Center for Molecular Medicine programme.

Author contributions

P.B.: design and execution of major experiments, collection of data, and interpretation and review of the manuscript; S.M.: execution of some experiments and collection of data; V.K.: execution of some experiments, collection of data, and review of the manuscript; A.R.: interpretation of some results and review of the manuscript; A.M.: concept and design of experiments, interpretation of results, manuscript writing, and final approval.

Disclosure of Potential Conflicts of Interest

The authors indicate no potential conflicts of interest.

References

1 Fattovich G, Stroffolini T, Zagni I et al. Hepatocellular carcinoma in cirrhosis: Incidence and risk factors. Gastroenterology 2004;127:S35–50.
2 Roberts MS, Angus DC, Bryce CL et al. Survival after liver transplantation in the United States: A disease-specific analysis of the UNOS database. Liver Transplant 2004;10:886–897.
3 Liu X, Hu H, Yi JQ. Therapeutic strategies against TGF-β signaling pathway in hepatic fibrosis. Liver Int 2006;26:8–22.
4 Liu Y, Wen XM, Lui ELH et al. Therapeutic targeting of the PDGF and TGF-β-signaling pathways in hepatic stellate cells by PTK787/ZK22258. Lab Invest 2009;89:1152–1160.
5 Schuppan D, Kim YO. Evolving therapies for liver fibrosis. J Clin Invest 2013;123:1887–1901.
6 Berardis S, Sattwika PD, Najimi M et al. Use of mesenchymal stem cells to treat liver fibrosis: Current situation and future prospects. World J Gastroenterol 2015;21:742–758.
7 El-Ansary M, Mogawer Sh, Abdel-Aziz I et al. Phase I trial: Mesenchymal stem cells transplantation in end stage liver disease. J Am Sci 2010;6:135–144.
8 Zhang Z, Lin H, Shi M et al. Human umbilical cord mesenchymal stem cells improve liver function and ascites in decompensated liver cirrhosis patients. J Gastroenterol Hepatol 2012;27:112–120.
9 Akihiro S, Yoshio S, Takuya K et al. Adipose tissue-derived stem cells as a regenerative therapy for a mouse steatohepatitis-induced cirrhosis model. Hepatology 2013;58:1133–1142.
10 Chiung-Kuei H, Soo OL, Kuo-Pao L et al. Targeting androgen receptor in bone marrow mesenchymal stem cells leads to better transplantation therapy efficacy in liver cirrhosis. Hepatology 2013;57:1550–1563.
11 Frank T, Henning WZ. Macrophage heterogeneity in liver injury and fibrosis. J Hepatol 2014;60:1090–1096.
12 Evaggelia L, Henning WZ, Ka-Kit L et al. Monocyte subsets in human liver disease show distinct phenotypic and functional characteristics. Hepatology 2013;57:385–398.
13 Lucia AP, Mark RT, Julia AW et al. Modulation of monocyte/ macrophage function: A therapeutic strategy in the treatment of acute liver failure. J Hepatol 2014;61:439–445.
14 Duffield JS, Forbes SJ, Constandinou CM et al. Selective depletion of macrophages reveals distinct, opposing roles during liver injury and repair. J Clin Invest 2005;115:56–65.

ID: parasuramank Time: 12:56 I Path: //chenas03/Cenpro/ApplicationFiles/Journals/Wiley/STEM/Vol00000/150206/Comp/APPFile/JW-STEM150206

15 Fallowfield JA, Mizuno M, Kendall TJ et al. Scar-associated macrophages are a major source of hepatic matrix metalloproteinase-13 and facilitate the resolution of murine hepatic fibrosis. J Immunol 2007;178:5288–5295.
16 Thomas JA, Pope C, Wojtacha D et al. Macrophage therapy for murine liver fibrosis recruits host effector cells improving fibrosis, regeneration, and function. Hepatology 2011; 53:2003–2015.
17 di Bonzo LV, Ferrero I, Cravanzola C et al. Humas MSCs as a two-edge sword in hepatic regenerative medicine: Engrafgtment and hepatic differentiation versus profibrogenic potential. Gut 2008;57:223–231.
18 Forbes SJ, Russo FP, Rey V et al. A significant proportion of myofibroblasts are of bone marrow origin in human liver fibrosis. Gastroenterology 2004;126:955–963.
19 Russo FP, Alison MR, Bigger BW et al. The bone marrow functionally contributes to liver fibrosis. Gastroenterology 2006;130: 1807–1821.
20 Group FMCS. Intraobserver and interobserver variations in liver biopsy interpretation in patients with chronic hepatitis C. The French METAVIR Cooperative Study Group. Hepatology 1994;20:15–20.
21 Yanez R, Lamana ML, Castro JG et al. Adipose tissue-derived mesenchymal stem cells have in vivo immunosuppressive properties applicable for the control of the graft-versus-host disease. STEM CELLS 2006;24:2582–2591.
22 Kochat V, Baliger P, Maiwal R et al. Bone marrow stem cells therapy in genetic and chronic liver diseases. Hepatol Inter 2014;8:166–178.
23 Usunier B, Benderitter M, Tamarat R et al. Management of fibrosis: The mesenchymal stromal cells breakthrough. Stem Cell Int 2014;2014:340257.
24 Waterman RS, Tomchuck SL, Henkle SL et al. A new MSC paradigm: Polarization into a pro-immflamatory MSC1 or an immunosuppressive MSC2 phenotype. PLoS One 2010;5: e10088.
25 Benyon RC, Arthur MJ. Extracellular matrix degradation and the role of hepatic stellate cells. Semin Liver Dis 2001;21: 373–384.
26 Pinzani M, Abboud HE, Gesualdo L et al. Regulation of macrophage colony-stimulating factor in liver fat-storing cells by peptide growth factors. Am J Physiol Cell Physiol 1992;262:C876–C881.
27 Cawston TE, Young DA. Proteinases involved in matrix turnover during cartilage and bone breakdown. Cell Tissue Res 2010; 339:221–235.
28 .Kisseleva T, Cong M, Paik H et al. Myofibroblasts revert to an inactivated phenotypes during regession of liver fibrosis. Proc Natl Acad Sci USA 2012;109:9448–9453.
29 Bataller R, Brenner DA. Liver fibrosis. J Clin Invest 2005;115:209–218.
30 Radaeva S, Sun R, Jaruga B et al. Natural killer cells ameliorate liver fibrosis by killing activated stellate cells in NKG2D-dependent and tumor necrosis factor-related apoptosis-inducing ligand-dependent manners. Gastroenterology 2006;130:435–452.
31 Taimr P, Higuchi H, Kocova E et al. Activated stellate cells express the TRAIL receptor-2/death receptor-5 and undergo TRAIL-mediated apoptosis. Hepatology 2003; 37:87–95.
32 Carvalho AB, Quintannilha LF, Dias JV et al. Bone marrow multipotent MSCs do not reduce fibrosis or improve function in a rat model of severe chronic liver injury. STEM CELLS 2008;26:1307–1314.
33 Knittel T, Kobold D, Saile B et al. Rat liver myofibroblasts and hepatic stellate cells: Different cell populations of the fibroblast lineage with fibrogenic potential. Gastroenterology 1999;117:1205–1221.
34 Rehman J, Traktuev D, Li J et al. Secretion of angiogenic and antiapoptotic factors by human adipose stromal cells. Circulation 2004;109:1292–1298.
35 Johnson TV, Martin KR, Tomerav SI. Platelet-derived growth factor-BB is involved in mesenchymal stem cell secretome-induced neuroprotection of retinal ganglion cells. Brain 2014;137:e276.
36 Liu CH, Hwang SM. Cytokine interactions in mesenchymal stem cells from cord blood. Cytokine 2005;32:270–279.
37 Issa R, Williams E, Trim N et al. Apoptosis of hepatic stellate cells: Involvement in resolution of biliary fibrosis and regulation by soluble growth factors. Gut 2001;48: 548–557.
38 Gao B, Radaeva S, Jeong WI. Activation of natural killer cells inhibits liver fibrosis: A novel strategy to treat liver fibrosis. Expert Rev Gastroenterol Hepatol 2007;1:173–180.
39 Muhanna N, Abu Tair L, Doron S et al. Amelioration of hepatic fibrosis by NK cell activation. Gut 2011;60:90–98.
40 Rastogi A, Maiwall R, Bihari C et al. Two-tier regenerative response in liver failure in humans. Virchows Arch 2014;464:565–573.
41 .Bird TG, Lu E-Y, Boulter L et al. Bone marrow injection stimulates hepatic ductular reactions in the absence of injury via macrophages-mediated TWEAK signaling. Proc Natl Acad Sci USA 2013;110:654–6547.
42 Newsome PN, Johannessen I, Boyle S et al. Human cord blood-derived cells can differentiate into hepatocytes in the mouse liver with no evidence of cellular fusion. Gastroenterology 2003;124:1891–1900.
43 Jang YY, Collector MI, Baylin SB et al. Hematopoietic stem cells convert into liver cells within days without fusion. Nat Cell Biol 2004;6:532–539.
44 Khurana S, Mukhopadhyay A. Characterization of the potential subpopulation of bone marrow cells involved in the repair of injured liver tissue. STEM CELLS 2007;25:1439–1447.
45 Yadav N, Kanjirakkuzhiyil S, Kumar S et al. The therapeutic effect of bone marrow-derived liver cells in the phenotypic correction of murine hemophilia A. Blood 2009; 114:4552–4561.
46 Vassilopoulos G, Wang PR, Russell DW. Transplanted bone marrow regenerates liver by cell fusion. Nature 2003;422:901–904.
47 Wang X, Willenbring H, Akkari Y et al. Cell fusion is the principal source of bone-marrow-derived hepatocytes. Nature 2003; 422:897–901.
48 Alvarez-Dolado M, Pardal R, Garcia-Verdugo JM et al. Fusion of bone-marrow-derived cells with Purkinje neurons, cardiomyocytes and hepatocytes. Nature 2003;425: 968–973.
49 Duncan AW, Hickey RD, Paulk NK et al. Ploidy reductions in murine fusion-derived hepatocytes.PLoS Gen 2009;5:e1000385.

See www.StemCells.com for supporting information available online.

AQ1: Please provide dept/div name (if any) for affiliation "a" and also confirm whether the affiliations are OK as given.

AQ2: Per journal style, most nonstandard abbreviations must be used at least two times in the abstract to be retained; MMP, IGF-1, and TGFβ were used once and have thus been deleted.

AQ3: Please provide the locations (city/state if within the US, and city/country if outside the US) and URLs for all manufacturer names mentioned in the experimental section.

AQ4: Please spell out PBS, FBS, PFA, IHC, DR, and LSK in the text.

AQ5: Per journal style, most nonstandard abbreviations must be used at least twice in the text to be retained; DMEM, DAPI, ALT, DCs, VEGF, and IVC were used only once and have thus been deleted.

AQ6: Please confirm whether the insertion of "Conclusion" section is OK as given.

AQ7: Please note that "**" has been depicted in Figure 4, but the significance of the same is not present in the corresponding legend. Please check.

AQ8: Please confirm that given names (red) and surnames/family names (green) have been identified correctly.